Indian Journal of Pure & Applied Physics
Vol. 53, January 2015, pp. 42-48

Structural and optical studies of Fe_2O_3 doped barium strontium titanate borosilicate glasses

Avadhesh Kumar Yadav*[2] & C R Gautam[1]

[1]Department of Physics, University of Lucknow, Lucknow 226 007, India

[2]Department of Physics, Indian Institute of Technology (BHU), Varanasi 221 005

*E-mail: yadav.av11@gmail.com

Received 21 August 2013; revised 8 October 2014 ;accepted 24 November 2014

Perovskite (Ba,Sr)TiO_3 borosilicate glasses in the system 64[($Ba_{1-x}Sr_x$).TiO_3]-30[2SiO_2.B_2O_3]-5[K_2O]-1[Fe_2O_3] ($0.4 \leq x \geq 1.0$) were prepared by conventional melt-quench method. Synthesized glass samples were characterized by infrared and Raman spectroscopic techniques for their structural investigations while optical properties of these glasses have been studied by using UV-Vis NIR spectroscopy. These investigations confirm the absence of boroxol ring in glassy matrix. Optical band gap of barium strontium titanate borosilicate glasses lies in the range 2.48-2.87 eV and its density has been found to be in the range 2.70-3.12 g/cc.

Keywords: Infrared spectroscopy, Raman spectroscopy, UV-Vis NIR spectroscopy, Barium strontium titanate

1 Introduction

Glasses are inorganic product of fusion which are cooled to a rigid condition without crystallization and long range order of atoms are completely absent[1]. The structure of multi-component glasses can be described in a less straight forward way and the choice of binary systems seems advantageous for undertaking systematic studies[2,3]. The vibrational band's shape, intensities and their positions would be affected by different vibrations by composition variation. At fixed composition, the shape of the former band is found to be dependent on the substrate temperature during deposition. Insight into the "mixing" nature of these vapour-deposited glassy solids has been obtained from an analysis of the spectral distribution of Si-O-Si, B-O-B and B-O-Si bonds as a function of composition[4]. Borates and borosilicate glasses containing boron oxide have been widely used for optical lenses due to high refractive index and low dispersion characteristics[5]. Raman spectroscopy is a very useful tool to provide valuable information about impurities, internal stress, crystal symmetry and bond nature[6–9]. IR and Raman studies on lithium-potassium-borate glasses exhibited due to vibrational stretching of borate network of the BO_3 and BO_4 units placed in different structural groups[10].

Recently, the IR and Raman spectroscopic studies on glass system [(Ba_xSr_{1-x})O.TiO_2]-[2SiO_2.B_2O_3]-[K_2O].[La_2O_3], have been reported. The different absorption bands such as molecular water, hydrogen bonding, B-O-B bonding, B-O-Si linkage etc. occurred in different wavenumber regions. These absorption bands depend on variation of Ba/Sr ratio as well as doping concentration of La_2O_3. Here, La_2O_3 acts as network modifier for glasses while the borosilicate works as glass former. The metallic cations were observed in low wavenumber regions.. The spectroscopic studies of barium strontium titanate borosilicate glasses[11–15] with addition of Fe_2O_3, have already been investigated. In the present paper, the IR, Raman and UV-Vis NIR spectroscopy on BST borosilicate glass system 64[($Ba_{1-x}Sr_x$)TiO_3]-30[2SiO_2-B_2O_3]-5[K_2O]-1[Fe_2O_3], has been studied.

2 Experimental Details

High purity analytical reagent grade chemicals $BaCO_3$ (Himedia 99%), $SrCO_3$ (Himedia 99%), TiO_2 (Himedia 99%), SiO_2 (Himedia 99.5%), H_3BO_3 (Himedia 99.8%), K_2CO_3 (Himedia 99.9%), and Fe_2O_3 (Himedia 99.9%) were used for the preparation of various glasses and their glass ceramic samples. The batch of 20 g in appropriate amount of AR grade chemicals has been prepared. Appropriate amount of different reagents chemicals of raw materials, as per the composition of glasses, was properly calculated, weighed and mixed in an agate mortar using acetone as mixing medium and dried. The glass batches weighing of 20 g were melted in a high-grade alumina

crucible in open air atmosphere using a programmable electric furnace (Metrex Scientific Instruments (P) Ltd. New Delhi). The melting temperatures for different compositions were in the range 1050-1450°C. The melt was maintained at the melting temperature in the furnace for 10 min for refining and homogenization. The melt was poured into an aluminum mould and pressed by a thick aluminium plate and then immediately transferred into a preheated programmable muffle furnace for annealing at temperature 450°C for 3 h to remove the residual stresses due to temperature gradient, which is produced by rapid cooling. The glasses were cooled within the furnace after annealing.

Infrared spectroscopy (IR) is an important tool for understanding the structure and dynamics of amorphous materials. It is also used to assign the observed absorption peaks to the proper vibration of the atoms in geometric grouping. The spectra of solids, many variables can affect the absorption peaks position as well as absorbance and the assignment of vibrational peaks of the atoms are very difficult. Usually, the method of repeated occurrence is followed in analyzing the IR spectrum of solid materials. Infrared absorption/transmission spectra of the powdered glass samples mixed with KBr powder and pressed as pellets were recorded using JASCO FT/IR-5300 and Brucker FTIR Tensor-27 in the wavenumber range 400-4000 cm^{-1} at room temperature. IR spectra of the prepared glass samples show the various absorption bands in different wavenumber regions. These bands are the characteristics of various vibrational modes of borate network as well as metallic cations.

Raman spectroscopy is one of the powerful technique to investigate the structure of a material. In IR spectroscopy, the nature of the light matter interaction is not the same as in Raman spectroscopy and the fundamental differences between the two processes determine the selection rules, which control Raman or IR activity of normal mode of vibration. Interaction of IR radiation with a normal mode of vibration occurs only when the electric field of radiation oscillates with the same frequency as instant dipoles caused by atomic vibrations. A normal vibration is, therefore, IR active only if a change in the dipole moment of the vibration occurs and is one photon process, as only photon is absorbed. Therefore, IR spectra give additional information than Raman spectra by which the symmetries of normal modes of vibration of molecules and crystal lattices are determined. Micro Raman set-up, Renishaw, UK, equipped with a grating of 1800 lines/mm and Olympus (model MX-50) A/T was attached with spectrometer which focuses laser light into sample and collect the scattered light at 180° by scattering geometry. The 15.4 nm Ar^+ laser was used as an excitation source and GRAM-32 software for data collection. Raman spectra (RS) of powdered glass samples were also recorded in the wavenumber range 200-3500 cm^{-1}.

UV-visible absorption spectroscopy is a very useful technique to characterize the optical and electronic properties of different materials such as thin films, filters, pigments and glasses. Measurement of the optical band gap of glass sample is carried out using the data within range 200-1200 nm obtained by spectrophotometer. There is a sharp increase in absorption at energies close to the band gap that manifests itself as an absorption edge in the UV-visible absorption spectra. UV-vis spectroscopy of the sample was carried out using UV-visible spectrophotometer (Varian, Carry-50Bio). It measures the percentage of radiation in the different regions such as ultra-violet (200-400 nm), visible (400-800 nm) and near infrared (800-1200 nm) regions that is absorbed at each wavelength within ultra-violet, visible regions and near infrared. Optical transitions are basically two types, direct and indirect transitions. In these transitions, the electromagnetic radiation interacts with the electrons in the valence band which reaches to conduction band by gaining fundamental band gap. These transitions occur in both crystalline and amorphous semiconductor materials. These transitions are related with Mott and Davis relation. For photon energies just above fundamental edge, the relation between absorption coefficient (α) and photon energy is given below[16,17]:

$$\alpha = (h\nu - E_g)^n / h\nu \quad \ldots(1)$$

where A is a constant related to the extent of the band tailing, n = 1/2 for allowed direct transition, = 2 for allowed indirect transition, $h\upsilon$ is the photon energy and E_g is the optical band gap energy of the material. The absorption coefficient, α, was calculated at different photon energies by using the relation, $\alpha = A/d$, where A is the absorbance and d is the thickness of the samples.

The optical band gap, E_g, was calculated by extrapolating the linear parts of the curves to $(\alpha h\upsilon)^{1/2} = 0$ of curve $(\alpha h\upsilon)^{1/2}$ versus $h\upsilon$ and extrapolating for

the glass samples. In general, density strongly depends on the compositions and structure of the glass and glass ceramic samples. Density of the glass and glass ceramic samples was determined using Archimedes principle[18]. Distilled water was used as the liquid medium. Density of glass and glass ceramic samples were calculated using the formula:

$$\rho = \frac{(W_2 - W_1)}{(W_4 - W_1) - (W_3 - W_2)} \rho_w \quad \ldots(2)$$

where ρ is the density (g/cc), ρ_w the density of distilled water 1 g/cc, W_1 the weight of empty specific gravity bottle (g), W_2 the weight of specific gravity bottle with sample (g), W_3 the weight of specific gravity bottle with sample and distilled water (g) and W_4 is the weight of specific gravity bottle with distilled water (g).

3 Results and Discussion

3.1 Infrared Spectroscopy

IR spectra of glass samples BST5K1F0.4, BST5K1F0.6, BST5K1F0.8 and ST5K1F1.0 are shown in the Fig. 1(a-d) and the peak positions have been listed in Table 1. IR spectra of all glass samples consist of different absorption bands in the wavenumber range 400-5000 cm^{-1}. These bands are affected by doping of Fe_2O_3 as well as the variation of Ba/Sr ratio. The positions of these bands are shifted with compositions. A broad absorption band in the wavenumber range 3451-3456 cm^{-1} is observed in IR spectra for all glass samples but the position of this band slightly varies with composition. This absorption band occurs due to molecular water content inside the glassy network[19]. The absorption band near 2927 cm^{-1} occurs due to the hydrogen bonding[20-22]. The sharpness of this band decreases with increasing the content SrO. The absorption bands in the wavenumber range 1227-1652 cm^{-1} are occurred due to the asymmetric stretching relaxation of the B-O bonds of trigonal BO_3 units. Such types of vibrational modes were observed within wavenumbers 1200-1750 cm^{-1} range[23]. The doublet splitting was observed in IR pattern of glass sample BST5K1F0.4 in two bands positions at 1652 and 1635 cm^{-1}, but the band at 1652 cm^{-1} was not found for other glass samples except IR spectrum of BST5K1F0.4. The absorption band near 1635 cm^{-1} was shifted to some higher wavenumber side by increasing the content SrO. A broad absorption band at about 1364 cm^{-1} in all glass samples and a shoulder peak at 1227 cm^{-1} have also been observed in glass BST5K1F0.4. The band in the range 1020-955 cm^{-1} is attributed to a stretching vibration of B-O-Si linkage[4]. This band was found very broad and its broadness follows linear trend except IR pattern of glass sample BST5K1F0.6. A weak absorption band is observed near 715 cm^{-1} in IR spectra of all glass samples. This weak band was present due to the diborate linkage, B-O-B in the borate glassy network. In this linkage, both boron atoms are tetrahedrally coordinated with triborate super structural units[24,25]. This band has shifted towards lower wavenumber side with increasing SrO content. In these glass samples, no absorption band at 806 cm^{-1} was observed and it confirms the absence of boroxol ring in glassy network. The bands near 444 cm^{-1} were occurred due to vibrations of metallic cations in glassy matrix in the IR spectra of all glass samples. The similar bands were also present in IR spectra of $PbO\text{-}B_2O_3$ glass as well as barium-borate oxide glasses and attributed to the vibrations of Pb^{2+}, Ba^{2+} and Mn^{2+} cations[26-29]. Hence, network-modifying behaviour was observed in which these ions entered the interstices of the network. This supports our

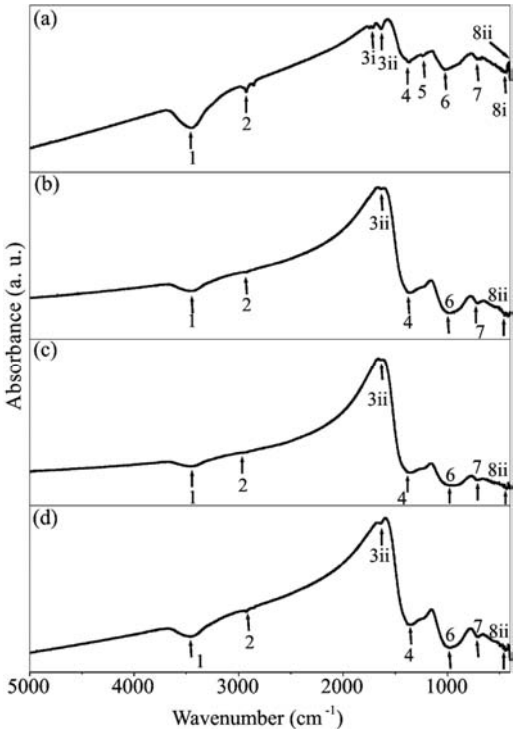

Fig. 1 — Infrared spectra of glass samples (a) BST5K1F0.4, (b) BST5K1F0.6, (c) BST5K1F0.8 and (d) ST5K1F1.0

Table 1 — Peak positions in IR spectra of glass samples in the system $64[(Ba_{1-x}Sr_x)TiO_3]$-30$[2SiO_2.B_2O_3]$-5$[K_2O]$-1$[Fe_2O_3]$

Glass sample code	Wavenumber of different absorption peaks (cm^{-1})									
	1	2	3		4	5	6	7	8	
			I	II					I	II
BST5K1F0.4	3451	2927	1652	1635	1368	1227	1020	716	452	444
BST5K1F0.6	3456	2927	-	1635	1364	-	984	715	-	443
BST5K1F0.8	3453	2928	-	1636	1367	-	955	712	-	444
ST5K1F1.0	3456	2927	-	1637	1360	-	984	712	-	441

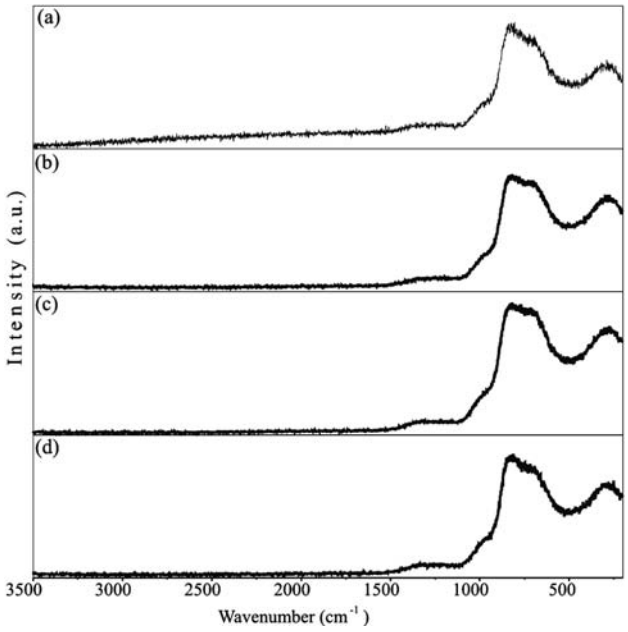

Fig. 2 — Raman spectra of glass samples (a) BST5K1F0.4, (b) BST5K1F0.6, (c) BST5K1F0.8 and (d) ST5K1F1.0

results and network-modifying behaviour of BaO and SrO was observed.

3.2 Raman Spectroscopy

Raman spectra of glass samples BST5K1F0.4, BST5K1F0.6, BST5K1F0.8 and ST5K1F1.0 are shown in Fig. 2(a-d) and peak positions of Raman spectra for these glass samples have been listed in Table 2. Raman spectra of all glass samples show four bands in wavenumber regions 1342-1322, 819-830, 712-722 and 279-288 cm^{-1}. The first observed Raman band in these glasses is due to the $B–O^-$ vibrations from various borate groups. Such types of bands were also found in IR spectra of BST borosilicate glass samples. The second band occurs due to symmetric breathing vibrations of six-member rings with one or two BO_3 triangles replaced by BO_4 tetrahedra and third observed Raman band was attributed to metaborate groups[30-34]. The spectral bands near 3450 and 2927 cm^{-1} are absent in Raman spectra due to the asymmetric change in dipole moment, thus IR active, but polarizability remains the same, Raman inactive. The band near 1342 cm^{-1} shifted lower wavenumber side with increasing the content of SrO. The positions of bands are observed with variation of Ba/Sr ratio. Raman shift from bands 823 cm^{-1} to 819 cm^{-1} increases with increasing the content of SrO from 40% to 60% while this band again shifted towards higher wavenumber with further in increasing the content of SrO from 60% to 80%. The position of Raman band at 722 cm^{-1} shifted towards lower wavenumber side with increasing the concentration of SrO up to 80 mole% but for pure Sr content glass sample, its position shifted towards higher wave-number side. The low frequency band near 288 cm^{-1} gives the similar behaviour as first Raman band. The assignment of IR and Raman bands in the spectra of different glass samples are summarized in Table 3.

Table 2 — Peak positions in Raman spectra of glass system $64[(Ba_{1-x}Sr_x).TiO_3]$-30$[2SiO_2.B_2O_3]$-5$[K_2O]$-1$[Fe_2O_3]$

Glass sample code	Raman band positions (cm^{-1})			
	1	2	3	4
BST5K1F0.4	1342	823	722	288
BST5K1F0.6	1332	819	718	282
BST5K1F0.8	1329	830	712	284
ST5K1F1.0	1322	825	716	279

3.3 UV-Vis NIR Spectroscopy

Figure 3 shows the UV-visible transmission spectra of glass samples BST5K1F0.4, BST5K1F0.6, BST5K1F0.8 and ST5K1F1.0. The absorption spectra of these glass samples do not show sharp absorption edge close to band gap. This characteristic of spectra is showing the amorphous nature of glass samples. Fig. 4 shows the Davis and Mott plot between $(\alpha h\upsilon)^{1/2}$ and photon energy ($h\upsilon$) for all glass samples. The band gap of BST borosilicate glass samples have been determined by extrapolation of linear part in Davis

Table 3 — Assignment of infrared and Raman bands in the spectra of various glass samples in glass system $64[(Ba_{1-x}Sr_x)TiO_3]$-30$[2SiO_2.B_2O_3]$-5$[K_2O]$-1$[Fe_2O_3]$

Wavenumber (cm^{-1}) IR	Raman	IR assignments	Raman assignments
441-452	279-288	Vibrations of metal cations such as Ba^{2+}, Sr^{2+}	Vibrations of metallic Cations
712-716	712-722	Bonding of B–O–B linkages (diborate linkage)	Symmetric breathing vibrations BO_3 triangles replaced by BO_4 tetrahedra
955-1020	819-830	Stretching vibration of B–O–Si linkage	Symmetric breathing vibrations of six-member rings with one or two BO_3 triangles replaced by BO_4 tetrahedra
1227-1652	1322-1342	Asymmetric stretching relaxation of the B–O bond of trigonal BO_3 units	$B–O^-$ vibrations
2927-2928	-	Hydrogen bonding	-
3451-3456	-	Molecular water	-

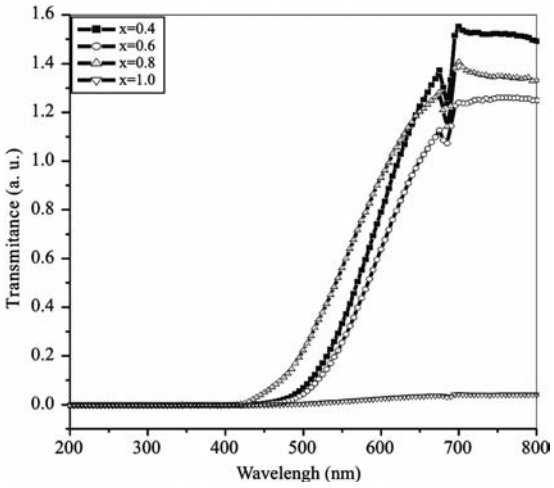

Fig. 3 — UV-Vis spectra of glass samples (a) BST5K1F0.4, (b) BST5K1F0.6, (c) BST5K1F0.8 and (d) ST5K1F1.0

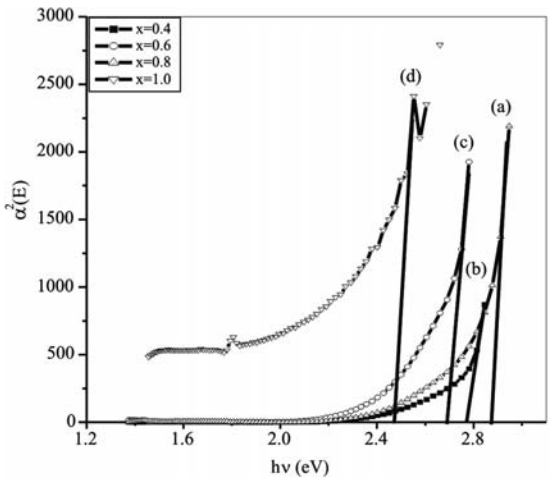

Fig. 4 — Davis and Mott plots of glass samples (a) BST5K1F0.4, (b) BST5K1F0.6, (c) BST5K1F0.8 and (d) ST5K1F1.0

Table 4 — Optical band gap and density of glass samples in the glass system $64[(Ba_{1-x}Sr_x).TiO_3]$-30$[2SiO_2.B_2O_3]$-5$[K_2O]$-1$[Fe_2O_3]$

Glass sample code	Optical band gap (eV)	Density (g/cc)
BST5K1F0.4	2.87	3.12
BST5K1F0.6	2.77	2.93
BST5K1F0.8	2.66	2.85
ST5K1F1.0	2.48	2.70

and Mott plots whereas the direct band gap was determined by extrapolation of linear part in Tauc plots as listed in Table 4.

The optical band gap E_g of these glasses varies with Ba/Sr ratio in the glass composition. The value of E_g was found to decrease with increasing the concentration of SrO. These results show the compositional dependence of optical band gap[35,36]. Such compositional dependence of optical band gap was followed by linear trend line as shown in Fig. 5. The optical band gap follows linear equation y_d=3.143-0.64x. The band gap varies from 2.48 to 2.87 eV. The similar results of band gap of $BaTiO_3$ were reported by Suzuki *et al.*, Piskunov *et al.*and Wemple *et al.*[37,38].

3.4 Density Studies

The density of glass and glass ceramics was determined by the liquid displacement method in the system $64[(Ba_{1-x}Sr_x).TiO_3]$-30$[2SiO_2.B_2O_3]$-5$[K_2O]$-1-$[Fe_2O_3]$ and listed in Table 4. It was observed that the density of glass and glass ceramic samples was affected by various factors such as chemical constituents, internal structure and heat treatment process. The density of BST borosilicate glasses was

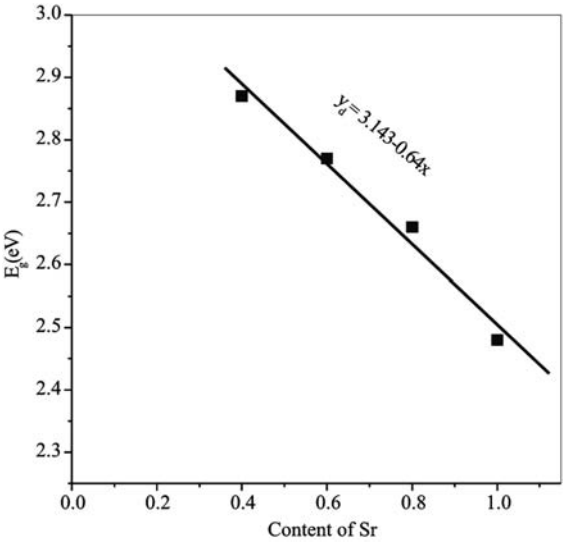

Fig. 5 — Variation of optical band gap with change of Ba/Sr ratio

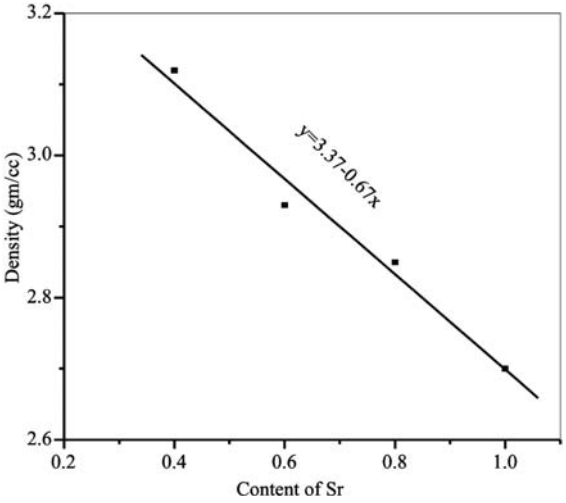

Fig. 6 — Variation of density of glasses with change in Ba/Sr ratio

found in the range 2.70-3.12 g/cc. The density of these glass samples is strongly influenced by Ba/Sr ratio. With increasing the content of SrO in glassy matrix, the density of BST borosilicate glasses decreases. This may be due to high density of Ba (3.51 g/cm^3) in comparison to Sr (2.61 g/cm^3). The density in Fe_2O_3 doping was slightly greater than La_2O_3 glass samples for the same composition, which may be due to high density of Fe (7.86 g/cm^3) to the La (6.51 g/cm^3). The variation of density with respect to composition change was shown in Fig. 6. The density follows the linear trend y=3.37-0.67x.

4 Conclusions

On the basis of above results on the study of structural and optical properties of barium strontium titanate glass ceramics in the glass system $64[(Ba_{1-x}Sr_x).TiO_3]$-$30[2SiO_2.B_2O_3]$-$5[K_2O]$-$1[Fe_2O_3]$ ($0.4 \leq x \leq 1.0$), it can be concluded as: (i) The BST borosilicate glasses were formed by various structural groups and confirmed by the combined study of infrared and Raman spectroscopy. Such types of structural groups are dominant in different wavenumber regions. The metal cations Ba^{2+}, Sr^{2+} are effective in low wavenumber side in IR spectra of these glasses. Here, the ferric oxide acts as the network modifier of these BST borosilicate glasses. (ii) The optical band gap of BST borosilicate glasses was in the range 2.48-2.87 eV. It is interesting that the Fe_2O_3 plays an important role that it decreases the optical band gap of barium strontium titanate borosilicate glasses. (iii) The density of BST borosilicate glasses lies in the range 2.70-3.12 gm/cc. Its value decreases with increasing the content of SrO.

Acknowledgement

The authors are gratefully acknowledged to the University Grant Commission (UGC), New Delhi, India for financial support under Major Research Project F. No. 37-439/2009 (SR).

References

1 Yamane M & Asahara Y, *Glasses for Photonics*, Cambridge University Press, Cambridge, (2000).
2 Mc Millan P F, *Am Mineralogy,* 69 (1984) 622.
3 Mc Millan P F & Wolf G H, *Am Mineralogy*, (eds) J F Stebbins (1995).
4 Tenney A S & Wong J, *J Chem Physics*, 56 (1972) 5516.
5 El-Alaily N A & Mohamed R M, *Mater Sci Eng Bull*, 98 (2003) 193.
6 Robins L H, Kaiser D L, Rotter L D, Schenck P K, Stauf G T & Rytz D, *J Appl Phys*, 76 (1994) 7487.
7 Yuzyuk Yu I, Farhi R, Lorman V L, Rabkin L M, Sapozhnikov L A, Sviridov E V & Zakharchenko I N, *J Appl Phys*, 84 (1998) 452.
8 Naik R, Nazarko J J, Flattery C S, Venkateswaran U D, Naik V M, Mohammed M S, Auner G W, Mantese J V, Schubring N W, Micheli A L & Catalan A B, *Phys Rev B*, 61 (2000) 11367.
9 Sirenko A A, Akimov I A, Fox J R, Clark A M, Li H C, Si W & Xi X X, *Phys Rev Lett,* 82 (1999) 4500.
10 Dobal P S, Bhaskar S, Majumder S B & Katiyar R S, *J Appl Phys,* 86 (1999) 828.
11 Gautam C R, Yadav A K & Singh A K, *ISRN Ceramics*, 2012 (2012) 1.
12 Gautam C R, Yadav A K, Mishra V K & Vikram K, *Open J Non-metallic Materials*, 2 (2012) 47.

13 Yadav A K & Gautam C R, *Lucknow J Science*, 8 (2011) 25.
14 Yadav A K & Gautam C R, *Optics & Photonics Journal*, 3 (2013) 1.
15 Yadav A K, Gautam C R, A Gautam & Mishra V K, *Phase Trans*, 86 (2013) 1000.
16 Davis E A & Mott N F, *Phil Mag,* 22 (1970) 903.
17 Eraiah B, *Bull Mater Sci,* 29 (2006) 375.
18 Hiremath V A, Date S K & Kulkarni S M, *Bull Mater Sci,* 24 (2001) 1001.
19 Rhim S M, Hong S, Bak H & Kim O K, *J Am Ceram Soc,* 83 (2000) 1145.
20 Bray P G, *Interac of radia with solids*, New York, Plenum (1967).
21 Adams R V & Douglas R W, *J Soc Glass Tech*, 43 (1959) 147.
22 Dunken H & Doremus R H, *J Non-Cryst. Solids*, 92 (1987) 61.
23 Husung R D & Doremus R H, *J Mater Res*, 5 (1990) 2209.
24 Dwoeidari H, Zeid A & Damraway E I, *J Phys D: Appl Phys*, 24 (1991) 2222.
25 Pal M, Roy B & Pal M, *J Mod Phys*, 2 (2011) 1062.
26 El-Egili K, *Physica B*, 325 (2003) 340.
27 Toderas A, Toderas M, Filip S & Ardelean I, *J Optoelectr Adv Mat,* 6 (2012) 331.
28 Kamitsos E I, Karakassides M A & Cryssikos G D, *J Phys Chem,* 91(1987) 1073.
29 Fengfeng L, Mingxi Z, Guiqin H, Yi S, Zhigang L & Hongsheng L, *Rare Met,* 30 (2011) 298.
30 Meera B N & Ramakrishna J, *J Non-Cryst Solids*, 159 (1993) 1.
31 Meera B N, Sood A K, Chandrabhas N & Ramakrishna J, *J Non-Cryst Solids*, 126 (1990) 224.
32 Konijnendijk W L & Stevels J M, *J Non-Cryst Solids*, 18 (1975) 307.
33 Furukawa T & White W B, *J Mat Sci*, 15 (1980) 1648.
34 Griguta L & Ardelean I, *J Optoelectr Adv Mat*, 10 (2008) 256.
35 George H B, Vera C, Stehle C, Meyer J, Evers S, Hogan D, Feller S & Affatigato M, *Phys Chem Glasses*, 40 (1999) 326.
36 Sharma G, Thind K S, Arora M, Singh H, Manupriya & Gerward L, *Phys Status Solidi A*, 204 (2007) 591.
37 Mady H A, *J Appl Sci Res*, 7 (2011) 1536.
38 Samantaray C B, Sim H & Hwang H, *Physica B*, 351 (2004) 158.